JOURNAL OF MATERIALS SCIENCE 25 (1990) 1886–1894

Preparation and properties of uniform mixed and coated colloidal particles

Part V *Zirconium compounds*

BAR AIKEN, WAN PETER HSU, EGON MATIJEVIĆ
Department of Chemistry, Clarkson University, Potsdam, New York 13676, USA

Colloidal dispersions of uniform spherical particles of zirconium basic sulphate and zirconium oxy-basic carbonate were prepared by ageing zirconium sulphate solutions at elevated temperatures in the presence of urea. Different chemical compositions of the above products resulted when the ageing temperature was altered. Depending on the nature of the original solids, calcination at 800° C resulted in the formation of tetragonal or monoclinic zirconia. Under certain conditions a mixed phase, including cubic zirconia, has also been identified. The particle morphology was retained during these transformations. Coprecipitation in mixed solutions of zirconium and yttrium salts aged at 80° C yielded composite spherical particles of basic carbonate with a zirconium to yttrium ratio of the solid similar to that used in the initial solution. Zirconium basic sulphate particles coated with yttrium basic carbonate were prepared by ageing, in the presence of urea, a $Zr_2(OH)_6SO_4$ dispersion containing yttrium nitrate.

1. Introduction

Zirconium oxide is a widely used material in applications where the solids are exposed to high temperatures [1, 2]. This compound exhibits thermal instability as it forms three different crystal structures depending on the temperature, t – i.e., cubic zirconia at $t >$ 2370° C, tetragonal from 1100 to 2370° C and monoclinic at $t <$ 1100° C [3]. It has been shown, however, that in microcrystalline form the tetragonal phase exists at room temperature and may transform to monoclinic zirconia over the temperature range between 300 and 700° C, depending on the crystallite size, method of preparation, etc. [4–7]. Garvie advanced the hypothesis that the tetragonal form has a lower surface free energy than the monoclinic one, which should account for the above described observation [4]. Since the optical, thermal, mechanical and electrical properties of ZrO_2 depend on its structure [8, 9], uniform particles of a definite internal composition should be useful in controlling the properties of this material.

Numerous procedures have been reported on the production of either partially or fully stabilized zirconia. Many of these processes have used dopings, such as the incorporation of yttria. The techniques included melting and cooling a mixture of the oxides [10], dehydration of aqueous yttrium and zirconium sulphates using alcohol [11], high temperature hydrolysis [12], spray pyrolysis [13] and wet chemical preparation using organic precursors [14].

In this work amorphous powders of spherical zirconium basic sulphate and zirconium basic carbonate particles of narrow size distribution were obtained by precipitation from homogeneous solutions using urea as an additive. These powders crystallized on heating. Depending on temperature, the structure changed from amorphous to tetragonal, then to mixed tetragonal–monoclinic and, finally, to monoclinic, while the particles retained their spherical shape.

By forced hydrolysis of mixed solutions of zirconium and yttrium salts, mixed oxy-basic carbonate dispersions were generated. The composition of the particles depended on the relative concentrations of the solute reactants. Such composite particles also crystallized on thermal treatment of the powders.

Finally, zirconium basic sulphate particles were coated by yttrium basic carbonate using a procedure developed earlier [15].

2. Experimental procedure

2.1. Materials

Zirconium sulphate (Aldrich, 99.9% Reagent Grade $Zr(SO_4)_2 \cdot 4H_2O$ yttrium nitrate (TMI 100, $Y(NO_3)_3 \cdot 6H_2O$), polyvinylpyrrolidone (Sigma, PVP-40 K), HNO_3 (Dilute-It) and urea (Baker analysed) were used as-received.

2.2. Particle generation

Pyrex test tubes containing solutions of metal salts and urea were tightly closed with Teflon lined caps and placed in a forced convection oven at predetermined temperatures. After ageing for various periods of time, the tubes were quenched by cooling to room temperature and then pH measurements were made on selected samples. The resulting dispersions were centrifuged at 2000 r.p.m. for 10 min, the supernatant solution discarded, and the particles resuspended in doubly distilled water in an ultrasonic bath. This

0022–2461/90 $03.00 + .12 © *1990 Chapman and Hall Ltd.*

process was repeated five times and the precipitates purified were dried and stored in a desiccator.

The concentrations of zirconium ions, hydrogen ions, urea, and a protecting agent (polyvinylpyrrolidone, PVP), as well as the ageing time and temperature were systematically varied to determine their effect on the final composition and morphology of the products. Solids of mixed composition were obtained by the same procedure with solutions of both metal ions.

Uniformly coated zirconium basic sulphate powders were prepared by ageing at elevated temperatures aqueous dispersions, containing a sufficient amount of these particles in the presence of dissolved yttrium nitrate.

2.3. Analyses

The zirconium content of the particles was assayed by plasma emission spectroscopy at 343.82 nm, while the yttrium content was determined by atomic absorption spectroscopy at 410.2 nm.

The solids were also characterized by differential thermal analysis (DTA), X-ray diffraction, specific surface area (BET) determination, as well as infrared and Raman spectroscopy. Thermogravimetric data were obtained by heating a known weight of a sample at a fixed temperature for three hours in a Lindberg heavy-duty furnace. The sample was then removed, reweighed and returned to the furnace for treatment at a higher temperature.

The size distribution of spherical particles was determined either from electron micrographs or by light scattering using the polarization ratio method [16]. Electrophoretic mobilities of the particles were determined with a DELSA (Coulter Electronics) instrument. To maintain constant ionic strength, the solids were first dispersed in either a NaOH or HNO_3 ($0.010\,mol\,dm^{-3}$) solution and the pH adjusted as necessary by the addition of acid or base. The dispersions were aged for 3 to 5 h, followed by ultrasonic treatment before the measurements were taken.

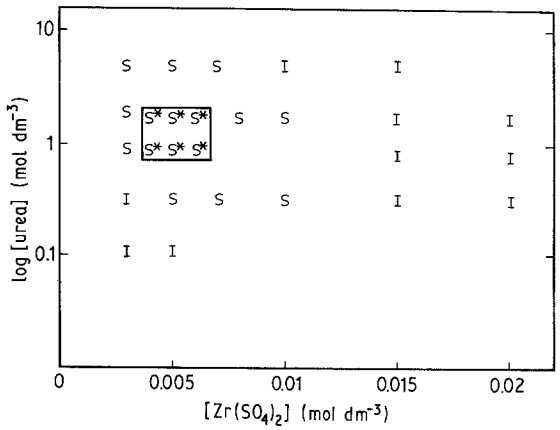

Figure 1 Precipitation domain for systems containing different concentrations of $Zr(SO_4)_2$ and urea, at constant concentrations of PVP (3% by weight) and HNO_3 ($5 \times 10^{-2}\,mol\,dm^{-3}$). Solutions were aged for 5 h at 50° C in sealed test tubes. Enclosed area represents conditions for the formation of uniform spherical particles. Symbols: S (spheres), S* (uniform spheres) and I (coagulated spheres).

3. Results

3.1. Preparation and characterization of colloidal Zr(IV) compounds

3.1.1. Preparation

A comprehensive study of the effect of the concentrations of the reactants (zirconium sulphate and urea) on the nature of the precipitated solids resulted in the

TABLE I Mean diameter of spherical zirconium containing particles obtained by ageing in capped tubes solutions containing $5.0 \times 10^{-2}\,mol\,dm^{-3}$ HNO_3 at 50° C (80° C)

a. Constant concentration: 3% PVP. Ageing time 5 h.

1. Concentration of urea: $1.8\,mol\,dm^{-3}$

$Zr(SO_4)_2$ concentration ($\times 10^3\,mol\,dm^{-3}$)	2.0	4.0	5.0	6.0	8.0	10
Particle diameter (μm)	0.32 (0.35)†	0.51 (0.39)	0.56(A)* (0.46)(B)*	0.61 (0.48)	0.81 (0.51)	0.80 (0.53)

2. Concentration of $Zr(SO_4)_2$: $5.0 \times 10^{-3}\,mol\,dm^{-3}$

Urea concentration ($mol\,dm^{-3}$)	0.45	0.90	1.35	1.80	2.25	
Particle diameter (μm)	0.49 (0.39)	0.52 (0.46)	0.54 (0.49)	0.56(A)* (0.46)(B)*	0.53 (0.47)	

b. Constant concentrations of $1.8\,mol\,dm^{-3}$ urea and $5.0 \times 10^{-3}\,mol\,dm^{-3}$ $Zr(SO_4)_2$

1. Concentration of: 3% PVP

Ageing time (h)	0.5	1.0	1.5	2.0	3.0	5.0	10	24
Particle diameter (μm)	0.38	0.49	0.50	0.53	0.54	0.56(A)*	0.57	(bimodal)

2. Ageing time: 5 h

PVP concentration (%)	0.5	1.0	1.5	2.0	2.5	3.0	4.0
Particle diameter (μm)	0.81	0.73	0.68	0.64	0.59	0.56(A)*	0.50

*Letters denote samples used in subsequent studies.

†Data in parentheses attained at 80° C.

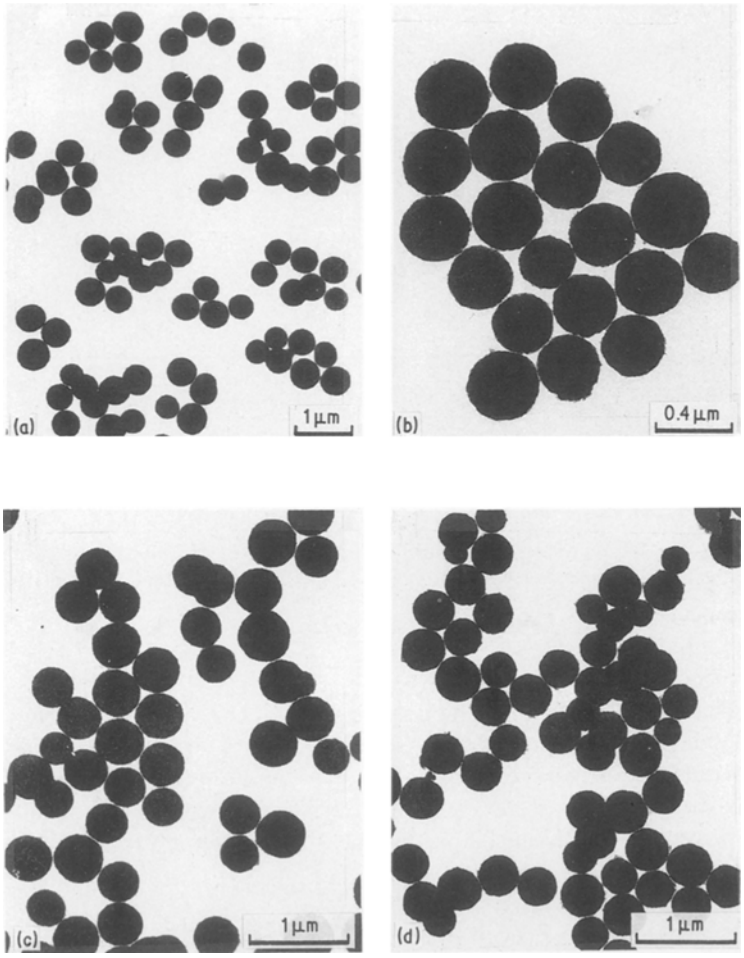

Figure 2 (a) Transmission electron micrographs (TEM) of particles obtained by ageing for 5 h at 50° C a solution 5×10^{-3} mol dm^{-3} $Zr(SO_4)_2$, 5×10^{-2} mol dm^{-3} HNO^{-3}, 1.8 mol dm^{-3} urea and 3% PVP (Table I, sample A). (b) As (a) calcined at 600° C for 3 h, (c) as (a) aged at 80° C for 5 h (Table I, sample B) and (d) as (c) calcined at 600° C for 3 h.

domain shown in Fig. 1. Data refer to systems aged at 50° C for 5 h in Teflon lined sealed tubes.

Dispersions consisting of spheres were obtained, over a given range of zirconium sulphate concentrations. The particles of greatest uniformity resulted under conditions delineated by the enclosed area in Fig. 1. The transmission electron micrograph (TEM) in Fig. 2a illustrates such a sample, designated A in Table I. All listed average particle diameters were obtained from electron micrographs.

The order of mixing the reagents was found to be important in preventing premature precipitation, which resulted in coagulated polydispersed particles. The following order of the addition of solutions yielded the most uniform particles: $Zr(SO_4)_2$, HNO_3, PVP, H_2O and urea. PVP was needed as a "protective agent", while HNO_3 lowered the pH of the original solution to ~2, thus delaying the onset of precipitation.

As summarized in Table I particle size increases with increasing concentration of the zirconium salt and decreasing concentration of PVP. Varying the content in urea between 0.45 and 2.25 mol dm^{-3} had little effect on the modal particle diameter. Finally, particle size remained essentially unchanged after ~2 h of interaction.

Outside the region of optimum conditions the size distribution broadened and the particle shape became somewhat distorted. Larger deviations from ideal conditions resulted in bimodal and/or agglomerated particles. Failure to use HNO_3 yielded polydisperse coagulated solids.

Identical solutions of $Zr(SO_4)_2$, aged at 80° C for 5 h, produced a similar precipitation domain. The transmission electron micrograph (Fig. 2c, sample B) shows that at higher temperatures the average particle size is smaller. (Note different size scale.) All other trends are the same as for systems generated at 50° C (Table I).

Exposure of samples A and B to a high energy beam in the electron microscope resulted in some shrinkage

TABLE II X-ray diffraction data for samples A, B, C and D calcined at 600° C (800° C) for 3 h

Sample A		Sample B		Sample C		Sample D	
d	I/I_0	d	I/I_0	d	I/I_0	d	I/I_0
2.94(3.13)	100(100)	2.93	100	4.09(2.97)	85(100)	(3.14)	(100)
1.82(2.83)	50 (63)	2.57	13	2.98(2.58)	100 (30)	(2.82)	(70)
1.80(2.61)	42 (44)	2.52	17	1.82(1.82)	31 (65)	(2.61)	(30)
1.55(1.53)	33 (37)	1.80	42	(1.55)	(37)	(1.81)	(60)
(1.84)	(37)	1.53	32				
(1.81)	(59)						

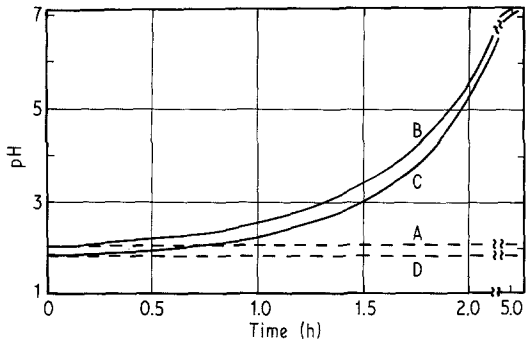

Figure 3 The change in pH as a function of time for solutions used to prepare samples A, B, C and D. Samples A and D were aged at 50° C while samples B and C were aged at 80° C.

with no other observable change. It was also noted that sample A was soluble in 1 mol dm^{-3} HNO_3 at room temperature while B was not. The initial and final pH for the solution used to prepare sample A was ~ 2, while for B the values were ~ 2.0 and 7.1, respectively (Fig. 3).

Calcination effects on representative powders were studied by heating the solids at predetermined temperatures in a furnace under air for 3 h (Table II). Electron micrographs of calcined samples A and B are given in Figs 2b and d, respectively. While some shrinkage took place, the particle morphology was retained. The total weight loss was ~ 42% and 29% for these samples at the final calcination temperature (T_c) of 800° C (Fig. 4).

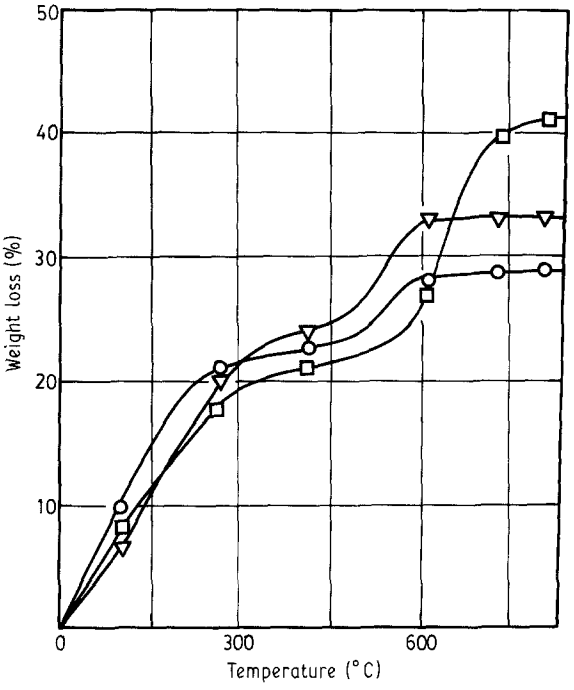

Figure 4 The change in weight as a function of temperature for samples A (□), B (○) and C (▽). The colours observed after calcination at different temperatures are as follows:

Sample	Calcination temperature (°C)							
	100	200	300	400	500	600	700	800
A	w	i	t	t	g	lg	w	w
B	w	i	t	lg	g	lg	w	w
C	w	i	i	t	g	lg	w	w

w (white), i (ivory), t (tan), g (grey), l (light).

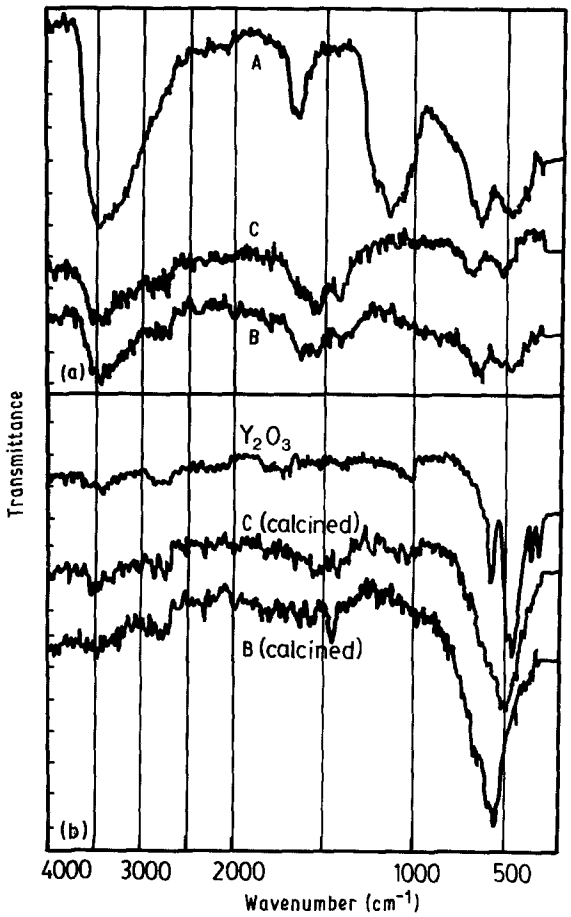

Figure 5 (a) Infrared spectra of samples A, B, (Table I) and C (Table III) and (b) infrared spectra of Y_2O_3 and samples B and C calcined at 800° C for 3 h.

3.1.2. Characterization

Quantitative microanalysis of sample A, stored in a desiccator at room temperature for three weeks, yielded 46.1% zirconium, 7.85% sulphur, 2.44% hydrogen and traces of carbon, corresponding to $Zr_2(OH)_6SO_4 \cdot 2H_2O$. This result is in good agreement with the known basic zirconium sulphates of a general formula $Zr_n(OH)_{2n+2}(SO_4)_{n-1}$ ($n > 1$) [17]. The analysis of sample B gave 50.6% zirconium, 3.42% carbon, 2.68% hydrogen and a trace of sulphur which is consistent with $Zr_2O_2(OH)_2CO_3 \cdot 2H_2O$. Weight losses on calcination of samples A and B given above are concordant with the change of these powders to ZrO_2.

In agreement with the chemical analysis, infrared spectra of A (Fig. 5a) show OH stretching vibrations (3000 to 3500 cm^{-1}), water of hydration band (1650 cm^{-1}) and sulphate bands (1070 to 1200 cm^{-1}, 570 to 670 cm^{-1}) [18, 19]. The spectrum of B (Fig. 5a) is, however, characteristic of a hydrated basic zirconium carbonate; the OH and water of hydration bands (3000 to 3500 and 1650 cm^{-1}, respectively) appear as well as the carbonate bands (1350 to 1600 cm^{-1}, 860 to 880 cm^{-1}) [20]. The powders of A and B (Fig. 5b) calcined at 800° C have the spectral characteristics of a monoclinic and tetragonal ZrO_2 polymorph, with a strong broad band at 530 cm^{-1} along with weak bands at 740, 640, 420 and 375 cm^{-1} [7, 21].

X-ray diffraction (XRD) data indicate that both samples (A and B) remain amorphous below 600° C.

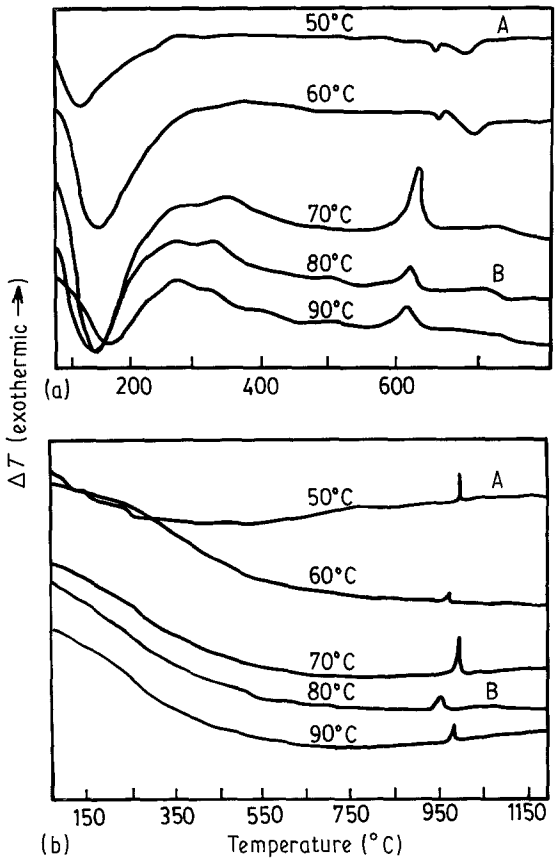

Figure 6 (a) Differential thermal analysis curves for samples prepared from solutions containing 5×10^{-3} mol dm^{-3} $Zr(SO_4)_2$, 5×10^{-2} mol dm^{-3} HNO_3, 1.8 mol dm^{-3} urea and 3% PVP aged in tightly sealed tubes for 5 h at: 50 (sample A), 60, 70, 80 (sample B) and 90° C. (b) DTA cooling curves for the same samples in the same order.

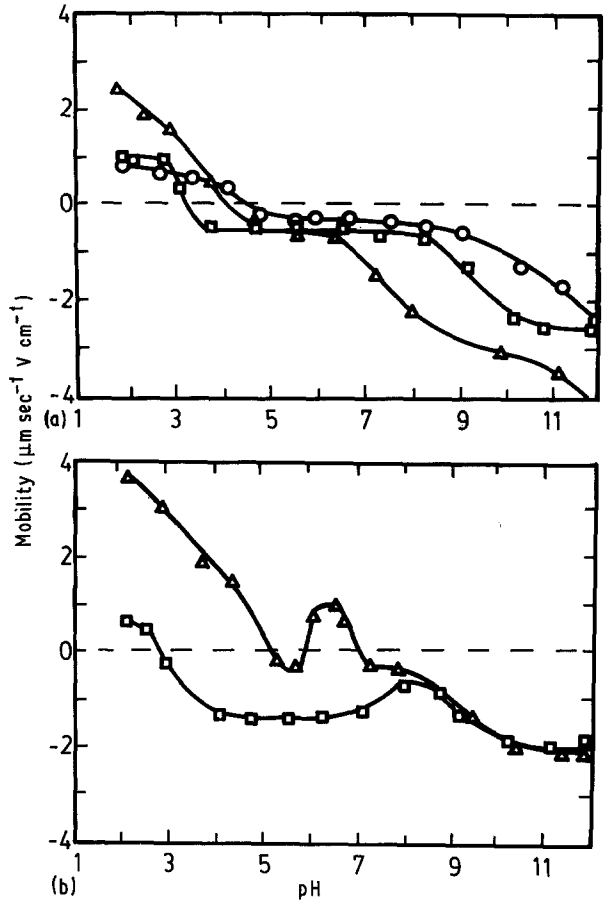

Figure 7 (a) Electrokinetic mobility of dispersions consisting of original samples A ($Zr_2(OH)_6SO_4$) (○), B ($Zr_2O_2(OH)_2CO_3$) (□) and calcined sample B (ZrO_2) (△) as a function of pH in 0.010 mol dm^{-3} $NaNO_3$. (b) Electrokinetic mobility of dispersions consisting of original sample C [$ZrY_{0.8}(OH)_{3.8}(CO_3)_{1.3}$] (□) and sample C calcined for 3 h at 800° C ($ZrY_{0.8}O_{3.2}$) (△) as a function of pH in 0.010 mol dm^{-3} $NaNO_3$.

Above this temperature the XRD pattern corresponds to crystalline tetragonal ZrO_2 [22]. Increasing the calcination temperature to 800° C did not alter sample B, while sample A indicated partial transformation to monoclinic ZrO_2 (Table II) [23]. Rinn and Schmidt also found that a change from tetragonal to monoclinic phase occurred at ~ 700° C in a zirconium compound formed by pyrolysis of zirconium alkoxides [7].

Raman spectra for samples A and B calcined at 700° C, show strong bands at 265, 470 and 645 cm^{-1}, as well as a moderate band at 330 cm^{-1} indicating tetragonal ZrO_2 structures for both samples.

Figure 6 (top) shows the DTA curves, obtained in air at a heating rate of 10° C min^{-1}, for samples prepared by ageing solutions described in the legend at temperatures ranging from 50 to 90° C. No transitions were observed between 800 and 1400° C during the same heating cycle. The DTA curves of samples prepared at the two lower temperatures display a broad endothermic peak (80 to 270° C) and an exothermic peak at 650° C located within a broad endothermic band ranging from 640 to 695° C [24]. Sample B exhibits additional exothermic peaks at 325 and 600° C. Based on the weight loss data, the first endothermic peak for sample A is due to the release of water of hydration [25], while for sample B this peak is a combined result of dehydration and carbonate decomposition [26]. The exothermic peak in sample A at 650° C indicates the transition to crystalline tetragonal zirconium oxide [7], while the endothermic band between 640 and 695° C represents the gradual decomposition of the sulphate [27]. The corresponding exothermic transition to crystalline tetragonal zirconium oxide takes place at a lower temperature (600° C) for sample B, while the exothermic peak at 325° C suggests the formation of crystalline $ZrO_{1.5}OH$. An exothermic reaction at similar temperatures has been reported in the transition of ammonium scandium carbonate to crystalline ScOOH [28]. A single X-ray diffraction peak at $d = 4.11$, found only in sample B calcined at 400° C, may be indicative of such a transition.

Cooling curves from DTA measurements (Fig. 6b) show the exothermic peak representing the monoclinic–tetragonal phase transformation at 980 and 1010° C for samples A and B, respectively, in agreement with previously reported data [29]. The specific surface area (SSA) of powder A was 5.5 m^2 g^{-1} and of sample B 8.7 m^2 g^{-1}. These relatively low values suggest non-porous solids.

The electrokinetic mobilities for aqueous suspensions of sample A give an isoelectric point (i.e.p.) at pH ~ 4.4 while calcined and uncalcined samples B had an i.e.p. of 3.4 and 4.2, respectively (Fig. 7a). It is difficult to compare these values with the reported literature data, since published i.e.p. for zirconia vary from 3 to

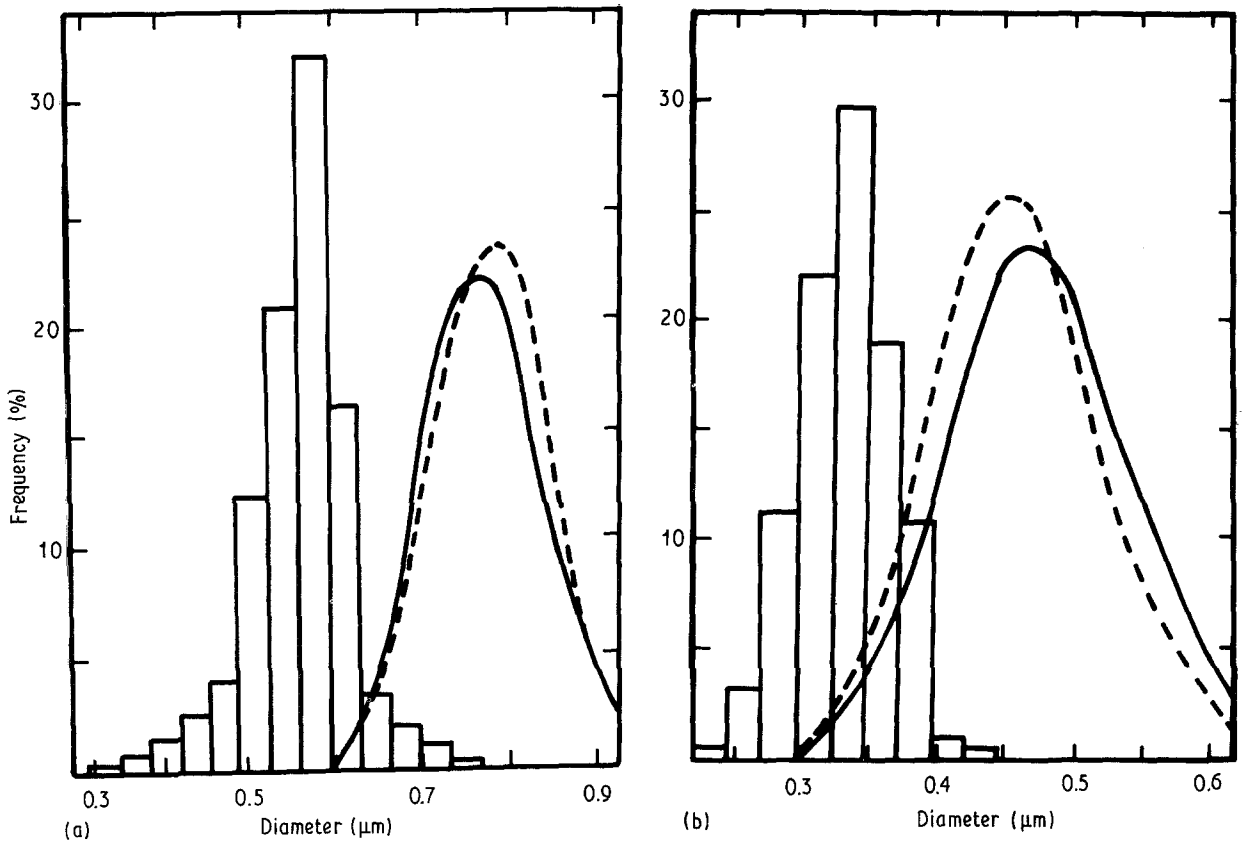

Figure 8 (a) Particle size distribution of $Zr_2(OH)_6SO_4$ sols (sample A, Fig. 2a) as determined by light scattering at 436 (– – –) and 546 (——) nm wavelengths (curves) and electron microscopy (histogram). (b) As (a) except the sol was produced by ageing for 3 h at 50° C a solution containing 5×10^{-3} mol dm^{-3} $Zr(SO_4)_2$, 5×10^{-2} mol dm^{-3}, HNO_3, 2.5×10^{-1} mol dm^{-3} urea and 1.75% PVP.

11.4, depending upon the source, method of preparation, purification procedure, etc. of this material [30, 31].

Figure 8 compares the size distribution of the $Zr_2(OH)_6SO_4 \cdot 2H_2O$ dispersion (sample A, Fig. 2a), as determined from a transmission electron micrograph (by counting between 300 and 500 particles) with that obtained by light scattering at 436 and 546 nm wavelengths using the polarization ratio method [16]. The latter yield a diameter ~ 40% larger than measured by electron microscopy. A duplicate run with another sample gave the same result. Obviously, considerable shrinkage of particles occurs on exposing this powder to the electron beam. The light scattering procedure also yields the refraction index of the investigated solids. The best fit of data was obtained with $n = 1.57$.

3.2. Preparation and characterization of particles of mixed Zr(IV)–Y(III) composition

3.2.1. Preparation

The transmission electron micrograph in Fig. 9a illustrates uniform spherical composite particles precipitated in solutions that were 5.0×10^{-3} mol dm^{-3} in $Zr(SO_4)_2$, 4.0×10^{-3} mol dm^{-3} in $Y(NO_3)_3$, 5.0×10^{-2} mol dm^{-3} in HNO_3, 3.0 wt % PVP and 1.8 mol dm^{-3} in urea aged at 80° C for 5 h in Teflon-lined capped tubes (sample C). Table III summarizes the effects of changing Zr^{4+}, Y^{3+} and urea concentrations. Attempts to incorporate yttrium ions at ageing temperatures below 80° C were unsuccessful as evidenced by chemical analysis, DTA curves and XRD data of the powder (Sample I) calcined at 800° C.

Addition of 1 mol dm^{-3} HNO_3 to a sample of these

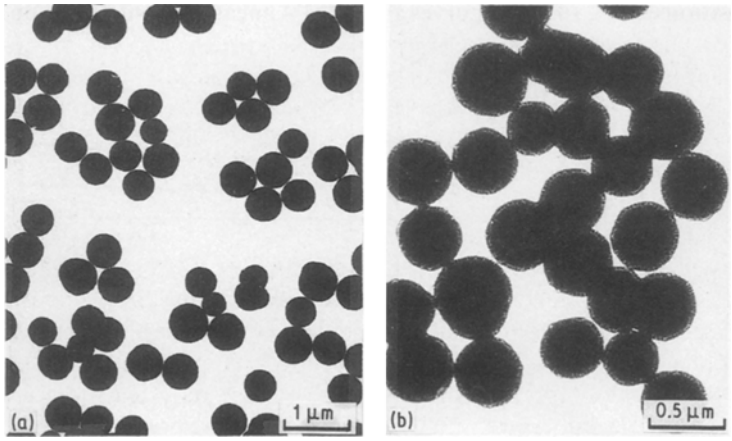

Figure 9 (a) TEM of particles obtained by ageing for 5 h at 80° C a solution 5×10^{-3} mol dm^{-3} $Zr(SO_4)_2$, 4×10^{-3} mol dm^{-3} $Y(NO_3)_3$, 1.8 mol dm^{-3} urea, 5×10^{-3} mol dm^{-3} HNO_3 and 3% PVP. (Table III, sample C). (b) TEM of $Zr_2(OH)_6SO_4$ particles coated with $Y(OH)CO_3$ prepared by heating for 2 h at 85° C a suspension of 0.3 g dm^{-3} $Zr_2(OH)_6SO_4$ containing 1×10^{-3} mol dm^{-3} $Y(NO_3)_3$ and 0.6 mol dm^{-3} urea. The coated particles were exposed to a high energy electron beam.

TABLE III Mean diameter of mixed Zr(IV)/Y(III) spherical particles obtained by ageing solutions containing 3% PVP and 5.0×10^{-2} mol dm^{-3} HNO_3 for 5 h at 80° C in capped tubes

a. Constant concentrations: 4.0×10^{-3} mol dm^{-3} $Y(NO_3)_3$ and 1.8 mol dm^{-3} urea						
$Zr(SO_4)_2$ concentrations ($\times 10^3$ mol dm^{-3})	2.0	4.0	5.0	6.0	8.0	10
Particle diameter (μm)	0.39	0.48	0.55(C)*	0.59	0.63	0.71
b. Constant concentrations: 5.0×10^{-3} mol dm^{-3} $Zr(SO_4)_2$ and 1.8 mol dm^{-3} urea						
$Y(NO_3)_3$ concentration ($\times 10^3$ mol dm^{-3})	2.0	4.0	6.0	8.0	10	
Particle diameter (μm)	0.52	0.55(C)*	0.59	0.60	0.57	
c. Constant concentrations: 5.0×10^{-3} mol dm^{-3} $Zr(SO_4)_2$ and 4.0×10^{-3} mol dm^{-3} $Y(NO_3)_3$						
Urea concentrations (mol dm^{-3})	0.45	0.90	1.35	1.80	2.25	
Particle diameter (μm)	0.46	0.57	0.53	0.55(C)*	0.59	

*Letter denotes sample used in subsequent studies.

composite particles resulted in partial dissolution, while some shrinkage was observed upon exposure to the high electron beam of the TEM. A weight loss of ~36% occurred on calcination to 800° C (Fig. 4).

3.2.2. Characterization

The chemical analysis of powder C, given in Table III is consistent with the composition $ZrY_{0.8}OH_{3.8}(CO_3)_{1.3} \cdot 0.8H_2O$, in agreement with the weight loss of 35% when calcined at 800° C to ZrO_2. The zirconium to yttrium content in the particles followed closely the initial composition of the reacting solution form which the solid was prepared. A dried powder showed infrared spectra before and after calcination at 800° C for 3 h (Fig. 5) that are characteristic of hydrated basic carbonate [20] and mixed metal oxide [21], respectively.

The X-ray diffraction pattern of the same sample revealed a mixed cubic–tetragonal ZrO_2 structure in agreement with results on yttria stabilized zirconia calcined at $\geqslant$ 800° C reported elsewhere [32, 33].

Differential thermal analysis (DTA) data for the composite sample C in air are compared with that of $Zr_2O_2(OH)_2CO_3 \cdot 2H_2O$ (sample B) and of $YOHCO_3 \cdot H_2O$ under the same conditions are given in Fig. 10. In the mixed system a broad doublet with maxima at 605 and 670° C indicates the presence of both metal ions. No further changes are noted on heating above 700° C. The cooling curve of the same sample C (Fig. 11b) shows no evidence of phase transformation,

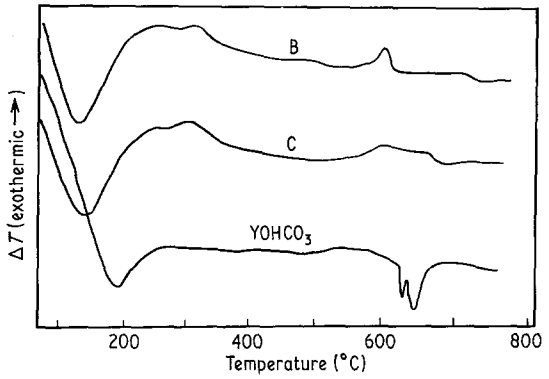

Figure 10 DTA curves for samples B (Table I), C (Table III) and $YOHCO_3$.

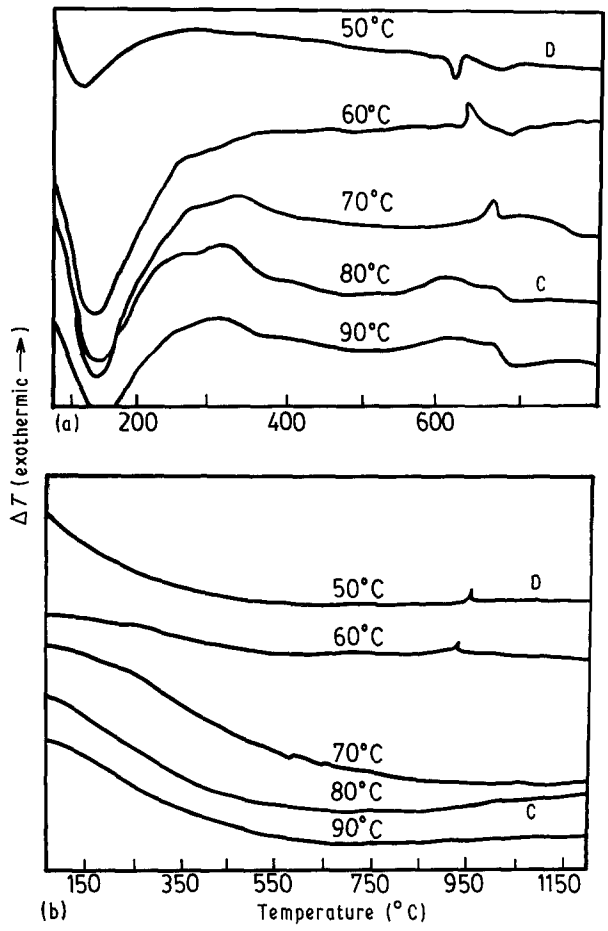

Figure 11 (a) DTA curves for samples prepared from solutions containing 5×10^{-3} mol dm^{-3} $Zr(SO_4)_2$, 4×10^{-3} mol dm^{-3} $Y(NO_3)_3$, 5×10^{-2} mol dm^{-3} HNO_3, 1.8 mol dm^{-3} urea and 3% PVP aged in tightly sealed test tubes for 5 h at: 50 (sample D), 60, 70, 80 (sample C) and 90° C. (b) DTA cooling curves for the same samples in the same order.

suggesting that calcination resulted in stable zirconium–yttrium mixed solids [34].

Electrophoretic mobilities of aqueous suspensions of powder C before and after calcination show different trends as a function of pH (Fig. 7b). The i.e.p. of the basic oxy carbonate is at pH = 2.7, whereas the same sample calcined at 670° C exhibits several isoelectric points, i.e., at pH 5.0, 5.7 and 6.8.

3.3. Preparation of Y(III) coated zirconium basic sulphate particles

To coat $Zr_2(OH)_6SO_4$ particles with yttrium compounds, 0.15 to 0.60 g dm^{-3} of this powder (sample A) was suspended in a solution of 1.0×10^{-3} to 4.0×10^{-3} mol dm^{-3} $Y(NO_3)_3$, containing 6.0×10^{-1} mol dm^{-3} urea, and the dispersion was then aged at 90° C for 2 h in tightly sealed Pyrex tubes.

Infrared spectroscopy confirmed that the coated layer consisted of $YOHCO_3$. As has been shown before [15, 24] $YOHCO_3$ decomposes in the high energy beam of the TEM resulting in a translucent layer which is easy to distinguish (Fig. 9b).

This thickness of the coating increased with the increasing ratio of $Y(NO_3)_3$ to the amount of solid particles; however, above a certain value excess yttrium basic carbonate precipitates as separate spheres in addition to the coated particles.

4. Discussion and conclusions

It has been reported [35, 36] that the rate of urea decomposition is temperature dependent with little change taking place below 75° C. Indeed, the pH of the reacting suspension aged at 50° C for 5 h remained constant at ~2.0. On addition of zirconium salts to aqueous solutions hydrated zirconium complexes, such as $Zr(OH)(H_2O)^{3+}$ are formed, although they are rarely found alone in aqueous solutions [37]. The hydrated ions undergo polymerization before reacting with sulphate ions according to

$$Zr_n(OH)_{2n+2}(H_2O)_n^{(n-1)2+} + (n-1)SO_4^{2-} \rightarrow Zr_n(OH)_{2n+2}(SO_4)_{n-1} + nH_2O \quad (1)$$

resulting in a general formula for basic zirconium sulphates [17]. The final product, from the sol of sample B, having a composition of $Zr_2(OH)_6SO_4 \cdot 2H_2O$, corresponds to $n = 2$.

Delays of the onset of precipitation on addition of nitric acid are to be expected, if the precursors to the solid phase formation involve hydrolysed cations coordinated with the sulphate ion [38]. Since urea does not decompose at 50° C, its effect on particle generation cannot be due to the release of OH^-. Instead, it is known that urea deactivates hydrogen ions [39], which in turn promotes hydrolysis and, consequently, nucleation and particle growth.

With increasing Zr^{4+} concentration, the diameter of the resulting spheres becomes significantly larger (Table Ia), indicating that the number of nuclei may have actually decreased. This might be the result of a lower initial pH of the solutions associated with the higher content in Zr^{4+}. To obtain optimum conditions for preparing uniform particles, at 50° C, a proper balance of urea–acid–$Zr(SO_4)_2$ components is necessary for controlling nucleation and particle growth processes (Fig. 1).

Polyvinylpyrrolidone (PVP) causes a decrease in the particle size (Table Ib) and the lesser degree of aggregation indicates that the polymer acts as a dispersant.

At higher ageing temperature of acidic solutions (80° C) the decomposition of urea yields ammonium ions and carbon dioxide [40, 41] causing an increase in the pH (Fig. 3). As a result the precipitation of zirconium basic carbonate, under these conditions can also be described by the overall reaction given in Equation 1, assuming that SO_4^{2-} is replaced by CO_3^{2-}, with $n = 2$. This mechanism is supported by studies showing that at pH > 4 the sulphate group, weakly coordinated by the metal ion, is easily replaced by other anions [37, 42, 43]. Since oxide instead of hydroxide bridging has been reported in suspensions of basic zirconium compounds at acidities lower than a few tenth molar [37], sample B may be better represented by $Zr_2O_2(OH)_2CO_3 \cdot 2H_2O$ rather than $Zr_2(OH)_6CO_3$.

As shown in Table Ia the average particle size of $Zr_2O_2(OH)_2CO_3$ sols increases with increasing $Zr(SO_4)_2$ concentration, suggesting that particle growth takes place after a relatively constant number of nuclei is formed, regardless of the amount of the zirconium ion present. Since the modal diameter of particles generated at 80° C is smaller than that at 50° C, after the same reaction times, it is assumed that the number of nuclei in the former case is larger.

In previous work on the preparation of lanthanide basic carbonate dispersions, it was reported that the [urea] to [metal ion] ratio in solutions determines the mean particle size [24]. In the present case, however, the particle size seems to be more strongly affected by the metal ion concentration. This difference may be attributed to the fact that much higher [urea] to $[Zr^{4+}]$ ratio is required to produce uniform spherical particles in zirconium sulphate solutions.

From the DTA (Fig. 6a) of amorphous powders of samples A and B, and the corresponding weight losses (given in parentheses) the following mechanisms of phase transformations are indicated:

Sample A

$$Zr_2(OH)_6SO_4 \cdot 2H_2O \xrightarrow{100^\circ C} \underset{(9\%)}{Zr_2(OH)_6SO_4} \xrightarrow{400^\circ C} \underset{(22\%)}{Zr_2O_3SO_4} \xrightarrow{700^\circ C} \underset{(41\%)}{2ZrO_2} \quad (2)$$

Sample B

$$Zr_2O_2(OH)_2CO_3 \cdot 2H_2O \xrightarrow{100^\circ C} \underset{(10\%)}{Zr_2O_2(OH)_2CO_3} \xrightarrow{250^\circ C} \underset{(23\%)}{Zr_2O_3(OH)_2} \xrightarrow{400^\circ C} \underset{(\text{crystal.})}{Zr_2O_3(OH)_2} \xrightarrow{600^\circ C} \underset{(28\%)}{2ZrO_2}. \quad (3)$$

Over the pH range 5 to 9 the negative charges of the sols A and B arise from the presence of coordinated anions such as sulphate or carbonate, which act as

stabilizing ions, in addition to the common potential-determining ions (H^+ and OH^-). The low constant mobility in this region may be attributed to the presence of positively charged hydrolysed zirconium complexes which compensate for some of the negative charge.

Precipitates formed in mixed solutions of $Zr(SO_4)_2$ and $Y(NO_3)_3$ aged at 50° C showed no presence of Y^{3+} (sample D), while those produced at 80° C had a composition corresponding to $ZrY_{0.8}OH_{3.8}(CO_3)_{1.3} \cdot H_2O$ with molar ratios of cations similar to their concentrations in the starting solution. These results, corroborated by the DTA (Fig. 11) and X-ray data, substantiate the mixed internal composition of the particles prepared by homogeneous precipitation. Table III shows the particle size to be sensitive to Zr^{4+} but not to Y^{3+} concentration. These data suggest that the Zr^{4+} ions initiate the nucleation stage, while Y^{3+} ions are incorporated into the particles during the subsequent growth.

The behaviour of particles of mixed composition (sample C) on heating show characteristics that are between those obtained with corresponding single cations (Fig. 4). The following changes in composition can be deduced from the DTA (Fig. 11a) and weight loss data

$$ZrY_{0.8}(OH)_{3.8}(CO_3)_{1.3} \cdot 0.8H_2O \xrightarrow{100^\circ C} \underset{(5\%)}{ZrY_{0.8}(OH)_{3.8}(CO_3)_{1.3}} \xrightarrow{250^\circ C} \underset{(22\%)}{ZrY_{0.8}O_{1.3}(OH)_{3.8}} \xrightarrow{600^\circ C} \underset{(33\%)}{ZrY_{0.8}O_{3.2}}. \quad (4)$$

XRD data from the calcined sample C revealed a mixed cubic–tetragonal ZrO_2, indicating that stabilized zirconia had been formed. Indeed, no phase change took place on cooling this solid. Electrokinetic mobilities of sample C in calcined form clearly show the effect of the presence of Y^{3+} in the mixed sample. The i.e.p. at pH 6.8 corresponds to that of pure Y_2O_3 [24].

Acknowledgement

E.M. was supported during this work by US Air Force contract F49620-85-C-0142.

References

1. S. M. HO, *Mater. Sci. Eng.* **54** (1982) 23.
2. D. J. CLOUGH, *Ceram. Engng Sci. Proc.* **6** (1985) 1244.
3. E. C. SUBBARAO, in "Advances in Ceramics", Vol. 3, edited by A. H. Heuer and L. W. Hobbs (The American Ceramic Society, Columbus, Ohio, 1983).
4. R. C. GARVIE, *J. Phys. Chem.* **69** (1965) 1238.
5. *Idem, ibid.* **82** (1978) 218.
6. M. A. BLESA, A. J. G. MAROTO, S. I. PASSAGGIO, N. E. FIGLIOLIA and G. RIGOTTI, *J. Mater. Sci.* **20** (1985) 4601.
7. G. RINN and H. SCHMIDT, "Preparation of Monodispersed Zirconia Powders from Solution", unpublished correspondence.
8. R. C. BUCHANAN and S. POPE, *J. Electrochem. Soc.* **130** (1983) 962.
9. T. MASAKI, *J. Amer. Ceram. Soc.* **69** (1986) 519.
10. B. H. DAVIS, *ibid.* **67** (1984) C-168.
11. M. P. O'TOOLE and R. J. CARD, *Amer. Ceram. Soc. Bull.* **66** (1987) 1486.
12. A. R. BURKIN, H. SARICIMEN and B. C. H. STEELE, *J. Brit. Ceram. Soc.* **79** (1980) 105.
13. H. ISHIZAWA, O. SAKURAI, N. MIZUTANI and M. KATO, *Amer. Ceram. Soc. Bull.* **65** (1986) 1399.
14. P. RECIO, C. PASCUAL, C. MOURE, J. R. JURADO and P. DURAN, *Brit. Ceram. Proc.* **38** (1986) 127.
15. B. AIKEN and E. MATIJEVIĆ, *J. Colloid Interface Sci.* **26** (1988) 645.
16. M. KERKER, "The Scattering of Light and Other Electromagnetic Radiation", (Academic Press, New York, 1969) pp. 351–373.
17. P. J. SQUATTRITO, P. R. RUDOLF and A. CLEARFIELD, *Inorg. Chem.* **26** (1987) 4240.
18. K. NAKAMOTO, "Infrared and Raman Spectra of Inorganic and Coordination Compounds" (John Wiley, New York, 1986) p. 248.
19. K. NAKANISHI and P. H. SOLOMON, "Infrared Absorption Spectroscopy", 2nd Edn (Holden-Day, San Francisco, 1977).
20. D. DOLPHIN and A. E. WICK, "Tabulation of Infrared Spectral Data" (John Wiley, New York, 1977).
21. N. T. McDEVITT and W. L. BAUN, *Spectrochem. Acta.* **20** (1962) 799.
22. "Powder Diffraction File, Inorganic Phases", No. 17-923, JCPDS International Center for Diffraction Data, Swarthmore, Pennsylvania (1981).
23. "Powder Diffraction File, Inorganic Phases", No. 13-307, JCPDS International Center for Diffraction Data, Swathmore, Pennsylvania (1981).
24. B. AIKEN, W. P. HSU and E. MATIJEVIĆ, *J. Amer. Ceram. Soc.* **71** (1988) 845.
25. G. GIMBLETT, A. A. RAHMAN and K. S. W. SING, *J. Chem. Tech. Biotechnol.* **30** (1980) 51.
26. T. L. WEBB and J. E. KRUGER, in "Differential Thermal Analysis", edited by R. C. MacKenzie (Academic Press, New York, 1970) p. 303.
27. J. P. REDFERN, *ibid.*, p. 148.
28. T. L. WEBB and J. E. KRUGER, *ibid.*, p. 311.
29. L. L. FEHRENBACHER, L. A. JACOBSEN and C. T. LYNCH, *Proc. Conf. Rare Earth Res.* **4**, Phoenix, Arizona, 1964.
30. G. A. PARKS, *Chem. Rev.* **63** (1965) 77.
31. G. W. SMITH and T. SALMON, *Can. Metall. Quart.* **5** (1966) 93.
32. K. S. MAZDIYASNI, C. T. LYNCH and J. S. SMITH, *J. Amer. Ceram. Soc.* **50** (1967) 532.
33. H. K. SCHMID, *ibid.* **70** (1987) 367.
34. P. DUWEZ, F. H. BROWN and F. ODELL, *J. Electrochem. Soc.* **98** (1951) 356.
35. G. J. BURROWS and C. E. FAWSITT, *J. Chem. Soc. (London)* **105** (1914) 609.
36. A. WERNER, *J. Chem. Soc.* **113** (1918) 84.
37. C. F. BAES and R. E. MESMER, "The Hydrolysis of Cations" (John Wiley, New York, 1976).
38. E. MATIJEVIĆ, K. G. MATHAI and M. KERKER, *J. Phys. Chem.* **66** (1962) 1799.
39. P. K. DAS GUPTA and S. P. MOULIK, *ibid.* **91** (1987) 705.
40. W. H. R. SHAW and J. J. BORDEAUX, *J. Amer. Chem. Soc.* **77** (1955) 4729.
41. R. C. WARNER, *J. Biol. Chem.* **142** (1942) 705.
42. H. H. WILLARD and H. C. FOGG, *J. Amer. Chem. Soc.* **59** (1937) 1197.
43. H. H. WILLARD and N. K. TANG, *ibid.* **59** (1937) 1190.

Received 1 June
and accepted 13 September 1988